

# A rapid compression machine and kinetic modelling study of 2-butanone

U. Burke<sup>\*,1</sup>, K. A. Heufer<sup>1</sup>

<sup>1</sup>Physico Chemical Fundamentals of Combustion, RWTH Aachen University, Schinkelstraße 8, 52062 Aachen, Germany

## Abstract

Oxygenated biofuels derived from biomass are being considered as possible replacements and/or supplements to current gasoline and diesel fuels. To date the most widely used of these is ethanol, however more and more potential oxygenated molecules are being synthesised from biomass. These molecules vary on a molecular structure level from ethers, to esters to ketones and many more. *This study* aims to provide engine relevant (high pressure 20-40 bar, and a wide range of temperatures) ignition delay time measurements which are used to develop and validate a chemical kinetic model. The rapid compression machine (RCM) used here has a single piston configuration with multiple access ports allowing for the measurement of pressure and light emission, in *this study* pressure has been used as a to define the ignition delay time. This RCM can be used to measure ignition delay times for compressed pressures of up to 150 bar. It has a heating system which allows for the study of low-volatility fuels, this can vary the initial temperature from ambient up to 200°C, in *this study* the system was heated to 50°C in order to be sufficient to prevent any condensation of 2-butanone. The combination of the experimental data and developed model allow for the elucidation of the underlying chemistry controlling the autoignition of 2-butanone. The data collected represent the first high-pressure and low-temperature measurements for 2-butanone. The model presented incorporates low-temperature chemistry reactions commonly associated with the low-temperature oxidation of *n*-alkanes. The experimental data measured for 2-butanone shows no negative temperature coefficient (NTC) behavior as seen in *n*-alkanes such as *n*-butane. This difference is attributed to the relatively fast, chain propagating HO<sub>2</sub> elimination pathways, due to the decrease in the bond strength energies of C–H bonds adjacent to the carbonyl group. Also the reduction in the bond strength of the C–C bonds adjacent to the carbonyl group also leads to relatively fast  $\beta$ -scission reactions compared to *n*-butane for example. The model has also been compared to experimental data available in the literature.

## Introduction

The increasing prevalence of global warming has caused the global community to actively search for viable ways to decrease its carbon footprint. To this end, the “Tailor Made Fuels from Biomass” (TMFB) cluster of excellence<sup>1</sup> at RWTH Aachen considers the process development (from well to wheel) and evaluation of biofuels implementation into the transport infrastructure. This approach is taken in response to the growing need to move away from the mass use of non-renewable fossil fuels and reduce harmful emissions associated with conventional fossil fuels. One of the solutions receiving much attention is the use of biomass to produce biofuels and thereby utilise these biofuels as transport fuels. A number of possible fuel classes have, and are being considered as possible biofuels such as alcohols, ethers and furans. Another class of compounds of interest is ketones. One of the ketones of interest is 2-butanone.

2-butanone has also been used as a fuel tracer compound for laser imaging diagnostics due to its ability to fluoresce<sup>2</sup>. It is necessary to consider the possible chemical effects these fuel tracers may have on the fuel mixture and therefore an understanding of the fundamental combustion chemistry is important.

These potential uses motivates the study of the fundamental combustion chemistry of 2-butanone. Some studies concerning the high-temperature

combustion of 2-butanone currently exist. Berckmüller *et al.*<sup>3</sup> used planar laser-induced fluorescence (PLIF) to study charge stratification in a lean burning spark-ignition engine. 2-butanone was used there, as a fuel tracer. Han and Steeper<sup>4</sup> used 2-butanone again as a fuel tracer while performing LIF. A microprobe coupled with gas chromatography was used by Gasnot *et al.*<sup>5</sup> to study the thermal degradation of 2-butanone under flame conditions. These measurements were also extended to consider the addition of 2-butanone to a methane in “air” flame. Lamoureux *et al.*<sup>6</sup> reported a reduction in NO<sub>x</sub> production when 2-butanone is added to a methane in “air” flame. The first ignition delay time study of 2-butanone was performed by Serinyel *et al.*<sup>7</sup>. These ignition delay times were performed at high temperatures (1250–1850 K), and used in the development and validation of a high temperature 2-butanone model. Recently this model has been updated by Badra *et al.*<sup>8</sup>, where new ignition delay times were measured in the temperature range of 1100–1400 K and at increased pressures than previously studied (3–6.5 atm). The study of Badra *et al.*<sup>8</sup> also measured the rate constants for 2-butanone+OH using laser absorption techniques in a shock tube. These rate constants have been previously investigated experimentally by Tranter *et al.*<sup>9</sup> and Lam *et al.*<sup>10</sup>. These same rate constants have been theoretically calculated, also reporting the individual abstraction site selectivity by Zhou *et al.*<sup>11</sup>.

\* Corresponding author: [burke@pcfc.rwth-aachen.de](mailto:burke@pcfc.rwth-aachen.de)

The hydrogen specific abstraction by hydroperoxyl radicals rate constants, have been theoretically calculated by Mendes *et al.*<sup>12</sup>. Lam *et al.*<sup>13</sup> reported high-temperature species-time histories in a shock tube for 2-butanone. From these measurements a new total rate constant for 2-butanone unimolecular decomposition was inferred from the species-time measurements.

Little or no studies have considered the oxidation of 2-butanone at low-temperatures, however the study of Sebbar *et al.*<sup>14</sup> calculated the thermochemistry and related reaction rate constants pertaining to the 2-butanone-3yl radical + O<sub>2</sub> potential energy surface.

Currently there no available detailed chemical kinetic models available in the literature which consider the low-temperature reaction kinetics associated with 2-butanone oxidation. In addition there have been no ignition delay time measurements made at combustion relevant regimes (> 10 bar). *This study* aims to rectify this by reporting ignition delay times at pressures of 20 and 40 bar and including a detailed chemical kinetic model which for the first time includes the low-temperature reaction rate constants necessary for the prediction of 2-butanone oxidation at low-temperatures.

## Experimental

The RCM used during the course of this study has been described in detail previously<sup>15</sup>. Briefly, it has a single piston configuration, with a variable volumetric ratio, which is possible through the interchange of the end walls (this alters the distance between the piston face and end wall). The RCM is equipped with a heating system covering the reactor chamber. This system is controlled and monitored by 13 thermocouples mounted along the reactor wall. This ensures a homogeneous initial temperature and also allows the RCM to study various initial temperatures (ambient up to 200°C). The ability to operate the RCM at different initial temperatures is specifically important when studying non-volatile fuels with low-vapour pressures where heating of the gaseous mixture maybe required in order to prevent condensation. Creviced piston heads, optimized to the facility's geometry, are used in order to suppress the formation of roll-up vortices and thereby ensuring a homogenous temperature field within the reactor core at the end of compression. The RCM has a 20% uncertainty in the measured ignition delay times. The pressure within the RCM is measured using a recessed and silicon coated PCB113B22 sensor. The compressed conditions were calculated using the compression/expansion routine in the Gaseq code<sup>16</sup>.

Butanone has been supplied by Sigma-Aldrich ( $\geq 99.0\%$ ). Oxygen ( $\geq 99.995\%$ ), argon ( $\geq 99.996\%$ ) and nitrogen ( $\geq 99.95\%$ ) were supplied by Westfalen AG and Praxair. Mixtures were premixed in two 1 L stainless steel heated mixing vessels. The mixtures were allowed to mix for at least 30 minutes in order to ensure homogenous mixing *via* gaseous diffusion.

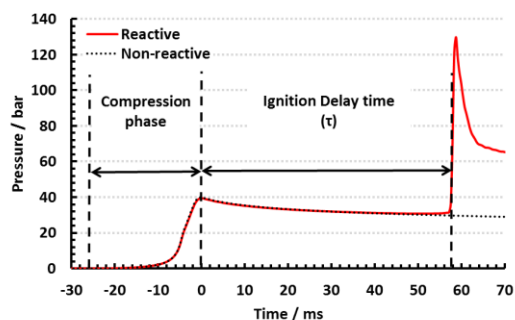


Figure 1: Typical pressure trace obtained during experiment. The definition of ignition delay time and a representative non-reactive trace, which was used for simulation is also shown.

Figure 1 presents a typical pressure trace obtained during the measurement of the ignition delay times presented here. Also highlighted in Fig.1 is the definition used for ignition delay time in all experiments. Ignition delay time was defined as the time between the end of compression (time = 0, when the piston has come to its final position) and the near instantaneous pressure increase caused by ignition. All experiments reported showed a near instantaneous pressure increase defining ignition similar to the example in Fig.1.

The developed chemical kinetic model was used to simulate the RCM experiments presented in *this study*. In order to simulate the data non-reactive experiments were taken concurrently with reactive experiments, where the O<sub>2</sub> concentration was exchanged for the similarly diatomic N<sub>2</sub>. This allowed quantification of the of the facility effects occurring during experiment. The facility effects during experiment can be considered firstly, as the finite time taken to compress the gaseous mixture (compression phase, Fig. 1) and secondly, as the facility effects post compression (flow into the crevice and heat losses to the walls) and occurring up to ignition. An example of a non-reactive experiment is shown in Fig. 1 (dotted black line). In order to accurately account for the change in pressure/temperature before and after compression the non-reactive profile is converted into an effective volume profile through the isentropic relationship between pressure and density thereby allowing the calculation of the effective volume. This allows the simulation to evolve the pressure and temperature parameters during simulation, both of which are important parameters when considering the chemical kinetics as the rate constants in the model can be both temperature and pressure dependent. This method of RCM simulation have been used previously in Burke *et al.*<sup>17</sup>, Darcy *et al.*<sup>18</sup> and Burke *et al.*<sup>19</sup>.

## Chemical Kinetic Model

A detailed chemical kinetic model is under development. The base chemistry used including thermodynamic data for the base species is taken from AramcoMech1.3<sup>20</sup>. The thermodynamic data for

butanone and all its related species including low-temperature species have been calculated here using quantum chemical calculations.

The rate constants for H-atom abstraction by hydroxyl and hydroperoxyl radicals have been adopted from the recent calculations of Zhou *et al.*<sup>11</sup> and Mendes *et al.*<sup>12</sup> respectively. Other H-atom abstractions from the sites adjacent to the carbonyl have been adopted as analogies to the rates proposed by Pelucchi *et al.*<sup>21</sup> for abstraction from a  $\beta$  and  $\gamma$  site in butanal. This analogy is made due to the similarities in the bond dissociation energies (BDEs). For butanal the BDEs for the  $\beta$  and  $\gamma$  sites are 91.9 and 97.9 kcal mol<sup>-1</sup> respectively, while for butanone the secondary and primary C–H bonds adjacent to the carbonyl site are 90.4 and 95.9 kcal mol<sup>-1</sup> respectively. The H-atom abstraction rate constants for the primary C–H on the 4-site on 2-butanone is taken as an analogy to the rate constants proposed in AramcoMech1.3<sup>20</sup> for abstraction from a primary site in butane, while correcting for degeneracy from butane to butanone.

The low-temperature reaction rate constants are assigned based on analogy to improved alkane rate rules<sup>22</sup>. However the reactions pertaining to the 2-butanone-3yl radical + O<sub>2</sub> potential energy surface have been adopted from the calculations of Sebban *et al.*<sup>14</sup>.

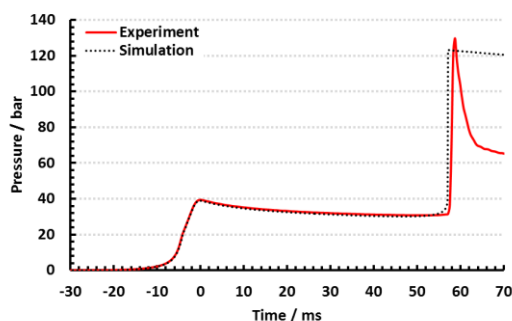


Figure 2: Example of a comparison of an experimentally measured pressure trace versus a pressure trace obtained through the RCM simulation method described in the text. Experimental conditions:  $\phi = 1.0$  in “air”,  $T_c = 861$  K,  $p_c = 40.35$  atm and  $\tau = 57.8$  ms.

Figure 2 introduces an example of a comparison of an experimentally measured pressure trace and a pressure trace obtained through the incorporation of an effective volume profile derived from the non-reactive pressure profile presented in Fig. 1. Note that the simulated pressure captures the changes in the experimental pressure during the compression phase and post-compression phase. In addition this figure also illustrates the excellent agreement between *this model* and experimental measurements, for this experimental example.

## Results and Discussion

As mentioned above low temperature (< 1000 K) ignition delay time measurements have been measured for the first time. 2-butanone in “air” mixtures at  $\phi = 1.0$

and compressed pressures of 20 and 40 bar are measured using a single-piston RCM. These results have been used to develop and validate the first 2-butanone detailed chemical kinetic model to include low-temperature oxidations pathways specific to 2-butanone. The experimental results and the results of the computational simulations are presented in Fig. 3.

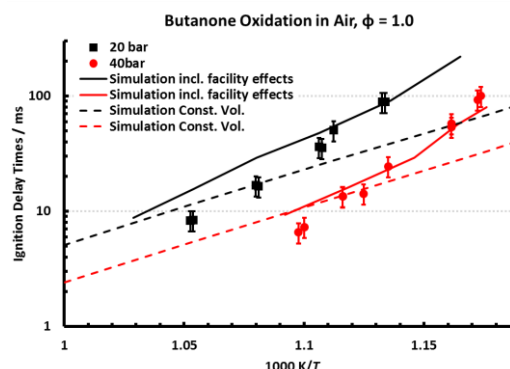


Figure 3: Experimental results versus model simulations for 2-butanone. Solid lines are simulations including RCM facility effects, dashed lines are constant volume simulations without the inclusion of facility effects.

Figure 3 shows that as compressed pressure increases ignition delay time decreases. The difference between the dashed and solid lines outlines the difference between simulating using a constant volume assumption versus simulation including the experimentally derived RCM facility effects. It can be seen that as ignition delay times get longer the heat loss effects post compression are most important and the data deviates to longer times than expected using a constant volume assumption. This effect is captured by the model in these cases and the model reproduces these data accurately. As the ignition delay times begin to decrease below 30 ms, the data begins to start to become shorter than the predicted constant volume simulations. This effect is accounted for by the increasing prevalence of chemical reaction during the compression stroke (hence the necessity to account for facility effects pre- and post-compression). In these cases the model over predicts ignition delay times and the deviation increases as the compressed temperature continues to increase. The model is in continued development in order to address the deviation seen in Fig. 3. But in order to provide some insight to the possible differences between predictions at the lower temperatures (883 K) and predictions at higher temperatures (950 K) flux analyses are compared describing prediction mechanism of oxidation moving from fuel decomposition, to fuel radical consumption reactions and finally the most abundant RO<sub>2</sub> species produced from the 2-butanone-3yl radical, how it is consumed (predicted by the model).

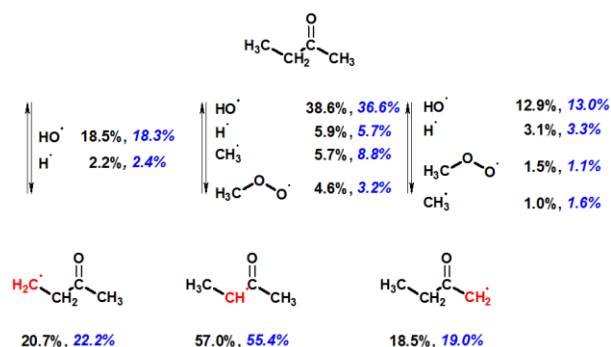


Figure 4: Flux analyses outlining the consumption reactions of butanone at  $T = 883$  K (black numbers) and  $950$  K (blue numbers). This was taken at  $20$  atm and for a  $\phi = 1.0$  in “air” mixture. The consumption reactions of 2-butanone are outlined.

Figure 4 presents flux analyses for  $\phi = 1.0$  in “air” at  $20$  atm and two temperatures  $883$  and  $950$  K. The flux analyses were performed when  $20\%$  of the initial fuel concentration had been consumed. There is no considerable difference shown in the mechanism of decomposition of 2-butanone predicted by the model from the lowest to the highest temperatures studied for  $20$  atm. It is notable that the favoured abstraction site is the secondary C–H bond adjacent to the carbonyl group (producing the 2-butanone-3-yl radical). This is to be expected considering it has the weakest bond strength.

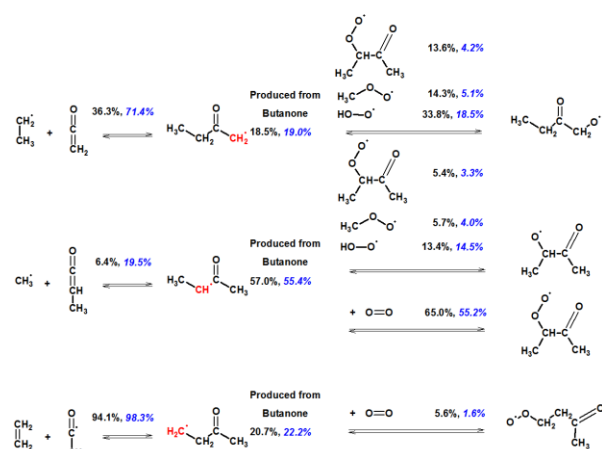


Figure 5: Flux analyses outlining the consumption reactions of butanone at  $T = 883$  K (black numbers) and  $950$  K (blue numbers). This was taken at  $20$  atm and for a  $\phi = 1.0$  in “air” mixture. The consumption pathways for the three possible fuel radicals are outlined.

The three radicals produced *via* H-atom abstraction from 2-butanone decompose through a number of competing reactions as outlined in Fig. 5. The most abundant radical from the initial fuel decomposition, 2-butanone-3-yl is primarily consumed at both the highest and the lowest temperatures studied through an  $\text{O}_2$  addition reaction. The flux of the 2-butanone-3-yl radical which favours the  $\beta$ -scission channel, over trebles moving from  $883$  K to  $950$  K. Significant amounts of the 2-butanone-3-yl and 2-butanone-1-yl radicals are consumed producing their respective  $\text{R}\dot{\text{O}}$  species. In

order to produce these  $\text{R}\dot{\text{O}}$  species the two specified radicals react with  $\text{HO}_2$ ,  $\text{CH}_3\text{O}_2$  and  $\text{CH}_3\text{O}_2\text{CHCOCH}_3$  radicals. The consumption of the 2-butanone-4-yl radicals are dominated by the  $\beta$ -scission channel forming acetyl radicals and ethylene. Due to the high quantity of  $\text{CH}_3\text{O}_2\text{CHCOCH}_3$  that builds in the system its reaction with both the 2-butanone-3-yl and 2-butanone-1-yl radicals is one of the consumption reactions of these radicals. For this reason the next consideration is the consumption of  $\text{CH}_3\text{O}_2\text{CHCOCH}_3$ .

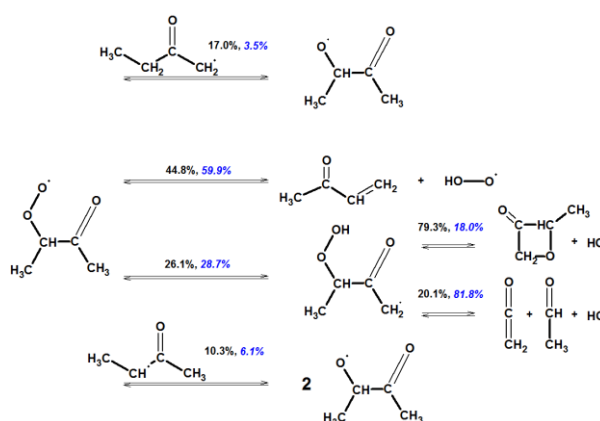


Figure 6: Flux analyses outlining the consumption reactions of butanone at  $T = 883$  K (black numbers) and  $950$  K (blue numbers). This was taken at  $20$  atm and for a  $\phi = 1.0$  in “air” mixture. The consumption reactions for  $\text{CH}_3\text{O}_2\text{CHCOCH}_3$  are outlined.

Figure 6 outlines the consumption reactions controlling the flux of  $\text{CH}_3\text{O}_2\text{CHCOCH}_3$ . The two minor pathways which decrease in importance as temperature increases are reaction with the 2-butanone-2-yl and 2-butanone-1-yl radicals forming  $\text{CH}_3\dot{\text{O}}\text{CHCOCH}_3$  (the relevant  $\text{R}\dot{\text{O}}$  species). The major consumption reactions are a  $\text{HO}_2$  elimination pathway producing  $\text{HO}_2$  radical and methyl vinyl ketone and, a 1, 5 H-atom shift internal isomerisation reaction forming the species,  $\text{CH}_3\text{HOOCHCOCH}_2$ . The product of the isomerisation reaction then proceeds either *via* a  $\beta$ -scission reaction resulting in the formation of ketene, acetaldehyde and hydroxyl radical or a ring closing reaction where a 4-membered cyclic ether is formed and a hydroxyl radical eliminated. As temperature increases the minor pathways outlined play less and less of a role and the two major pathways become even more dominant. In addition at higher temperatures the  $\text{HO}_2$ -elimination reaction becomes even more strongly favoured relative to the isomerisation reaction.  $\text{CH}_3\text{HOOCHCOCH}_2$  formed through the isomerisation reaction as mention either undergoes  $\beta$ -scission or forms a cyclic ether species, and through the flux analyses presented in Fig. 5 it is observed that as temperature changes from  $883$  K to  $950$  K the favoured consumption reaction changes from the cyclic ether formation to the  $\beta$ -scission reaction. This mechanism of oxidation of 2-butanone described above is similar to the mechanism of oxidation to current *n*-alkane predictions for compounds such as butane. However it differs in that

the reaction between radicals (R) and  $\text{HO}_2$ ,  $\text{CH}_3\dot{\text{O}}_2$  and  $\text{RO}_2$  consume more of the fuel radical species than what is observed for well-known *n*-alkanes.

Brute force sensitivity analyses were performed in order to determine the reaction rate constants that were controlling the prediction of ignition delay times in the current model. The sensitivity analyses were performed by simulating the specified condition while increasing and decreasing each rate constant in the model by a factor of 2. The sensitivity coefficient reported was then determined using the following equation:

$$S = \frac{\log_{10}(\tau_+/\tau_-)}{\log_{10}(k_+/k_-)} = \frac{\log_{10}(\tau_+/\tau_-)}{\log_{10}(2/0.5)}$$

Equation 1: Calculation of sensitivity coefficient.

Where  $\tau_+$  is the simulated ignition delay time when a rate constant is increased by a factor of 2,  $\tau_-$  is the simulated ignition delay time when a rate constant has been decreased by a factor of 2,  $k_+$  is the rate constant when it is doubled and  $k_-$  is the rate constant when it is halved. Therefore a negative sensitivity coefficient denotes a rate constant that is promoting reactivity, while a positive sensitivity coefficient denotes a rate constant that is inhibiting reactivity.

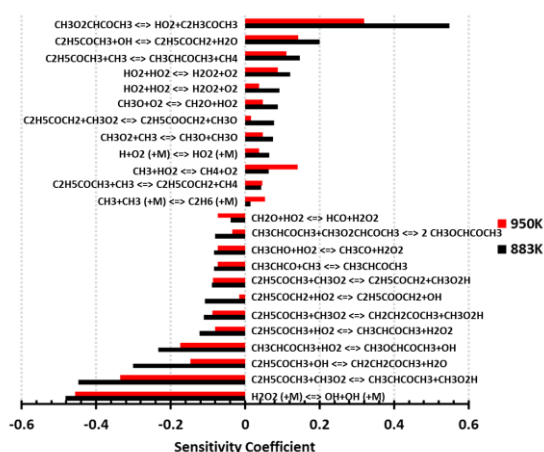


Figure 7: Sensitivity analysis performed for  $\phi = 1.0$  in “air”,  $T = 883$  and  $950$  K,  $p = 20$  atm.

Figure 7 presents the results of a sensitivity analysis calculated for a  $\phi = 1.0$  in “air” mixture at temperatures of  $882$  and  $950$  K and  $p = 20$  atm. Hydrogen peroxide decomposition is the most promoting reaction in both cases, which is not surprising considering it is a chain branching reaction and is a major source of hydroxyl radicals during oxidation. Also shown to be promoting are H-atom abstraction reactions by methylperoxy, hydroxyl and hydroperoxy radicals. These are promoting because as shown in Fig. 4 they are the main consumption reaction of 2-butanone. Both 2-butanone-3yl and 2-butanone-1yl radicals reaction with hydroperoxy radicals to form their respective  $\text{RO}$  species and hydroxyl radicals are seen to be promoting reactions. This is because they produce hydroxyl radicals and are consumption reactions of the fuel

radicals. The most inhibiting reaction for both cases is  $\text{HO}_2$  elimination from the  $\text{RO}_2$  species derived from 2-butanone-3yl.  $\text{HO}_2$  elimination is an inhibiting reaction because it competes with the possible isomerisation reactions which if favoured can lead to a second  $\text{O}_2$  addition and eventually production of 2 extra hydroxyl radicals (this is the common chain branching mechanism associated with the oxidation of *n*-alkanes). Interestingly H-atom abstraction by hydroxyl radical forming 2-butanone-1yl radical is the second most inhibiting reaction (decreasing to third most inhibiting as the temperature increases to  $950$  K). The reason that this fuel consumption reaction is inhibiting is that when the 2-butanone-1yl is formed it favours either the formation of its relevant  $\text{RO}$  or formation of ketene and ethyl radical through  $\beta$ -scission. If the fuel is consumed to form either 2-butanone-3yl or 2-butanone-4yl radicals the consumption reaction for these radicals yield more reactive species than the products of the consumption of 2-butanone-1yl radicals. In the case of 2-butanone-3yl  $\text{O}_2$  addition is favoured for both temperatures considered. While for 2-butanone-4yl  $\beta$ -scission is favoured and it yields ethylene and acetyl radicals, two species which are more reactive than the products produced from the  $\beta$ -scission of 2-butanone-1yl (ethyl radical and ketene).

There is not a huge change in the sensitive reactions as temperature increases from  $882$  K to  $950$  K. However the reaction  $\text{C}_2\text{H}_5\text{CO}\dot{\text{C}}\text{H}_2 + \text{HO}_2 \rightleftharpoons \text{C}_2\text{H}_5\text{COO}\dot{\text{C}}\text{H}_2 + \dot{\text{O}}\text{H}$  does become much less promoting as the temperature increases to  $950$  K. There is also an increase in the inhibiting effect of  $\dot{\text{C}}\text{H}_3 + \text{HO}_2 \rightleftharpoons \text{CH}_4 + \text{O}_2$  as the temperature increases from  $883$  K to  $950$  K. There is a significant decrease in the inhibiting effect of  $\text{CH}_3\dot{\text{O}}_2\text{CHCOCH}_3 \rightleftharpoons \text{HO}_2 + \text{C}_2\text{H}_5\text{COCH}_3$  as the temperature increases. This is likely due to the gradual decrease in the amount of 2-butanone-3yl radical being consumed via  $\text{O}_2$  addition.

## Conclusions

Ignition delay times have been measured in an RCM for the first time for 2-butanone. The data was taken for fuel in “air” mixtures at  $\phi = 1.0$ , covering compressed pressures of  $20$  and  $40$  atm and compressed temperatures of  $852$ – $950$  K. These data were used in order to develop and validate new detailed chemical kinetic model for the oxidation of 2-butanone. This model includes low-temperature reaction pathways which are based on the accepted mechanism of oxidation of alkanes.

While the experimental data presented showed now NTC behaviour, the prediction of the data was found to rely on many of the low-temperature reaction pathways included in the new model. For example the majority of the 2-butanone-3yl radical produced from 2-butanone was observed to be consumed by  $\text{O}_2$  addition. So while no NTC behaviour was seen in the data, in order to accurately predict the data inclusion of the low-temperature reaction pathways was necessary.

The model development is currently ongoing due to deviations between model predictions and experimental data at the higher temperatures studies ( $\approx 950$  K). In *this study* the possible reasons for these deviations are presented and discussed. What is found is an increased sensitivity to the reaction class,  $R+RO_2 \rightleftharpoons 2 RO$  relative to that seen for *n*-alkanes. In addition this reaction class is seen to reduce in importance (with regard to ignition delay time prediction) as the temperature increases. This may point to an erroneous temperature dependence in the current assignment of the rate constants for the reactions of this class for 2-butanone. In order to further test the model shock tube data for the mixtures presented in *this study* will be collected in order to improve the model development.

### Acknowledgements

This work was performed as part of the Cluster of Excellence "Tailor-Made Fuels from Biomass" which is funded by the Excellence Initiative of the German Federal State Governments to promote science and research at German Universities. The support from Prof. Kai Leonhard and Dr. Wassja Kopp of Lehrstuhl für Technische Thermodynamik (LTT) is greatly appreciated.

### References

1. <www.fuelcenter.rwth-aachen.de>, 2010.
2. C. Schulz, V. Sick, Prog. Energy Combust. Sci. 31 (2005) 75-121.
3. M. Berckmüller, N. P. Tait, R. D. Lockett, D. A. Greenhalgh, K. Ishii, Y. Urata, H. Umiyama, K. Yoshida, Proc. Combust. Inst. 25 (1994) 151-156.
4. D. Han, R. R. Steeper, 29 (2002) 727-734.
5. L. Gasnot, V. Decottignies, A. Turbiez, J. F. Pauwels, Combust. Sci. Tech. 161 (2000) 1-25.
6. N. Lamoureux, A. Bakali, L. Gasnot, J. F. Pauwels, P. Desgroux, 153 (2008) 186-201.
7. Z. Serinyel, G. Black, H. J. Curran, J. M. Simmie, Combust. Sci. Technol. 182 (2010) 574-587.
8. J. Badra, A. E. Elwardany, F. Khaled, S. S. Vasu, A. Farooq, 161 (2014) 725-734.
9. R. S. Tranter, R. W. Walker, Phys. Chem. Chem. Phys. 3 (2001) 1262-1270.
10. K. Lam, D. Davidson, R. Hanson, J. Phys. Chem. A, 116 (2012) 5549-5559.
11. C. -W. Zhou, J. M. Simmie, H. J. Curran, Phys. Chem. Chem. Phys. 13 (2011) 11175-11192.
12. J. Mendes, C. -W. Zhou, H. J. Curran, 117 (2013) 4515-4525.
13. K. -Y Lam, W. Ren, S. H. Pyun, A. Farooq, D. F. Davidson, R. K. Hanson, Proc. Combust. Inst. 34 (2013) 607-615.
14. N. Sebbar, J. W. Bozzelli, H. Bockhorn, Z. Phys. Chem. 225 (2011) 993-1018.
15. C. Lee, K. A. Heufer, S. Vranckx, S. Medvedev, S. Khomik, Y. Uygun, H. Olivier, R. X. Fernandes, Z. Phys. Chem. 226 (1) 2014, 1-27.
16. C. Morley, GasEq, Version 0.76, 2004, <<http://www.gaseq.co.uk>>.
17. U. Burke, K. P. Somers, P. O'Toole, C. M. Zinner, N. Marquet, G. Bourque, E. L. Petersen, W. K. Metcalfe, Z. Serinyel, H. J. Curran, 162 (2015) 315-330.
18. D. Darcy, H. Nakamura, C. J. Tobin, M. Mehl, W. K. Metcalfe, W. J. Pitz, C. K. Westbrook, H. J. Curran, 161 (2014) 1444-1459.
19. S. M. Burke, U. Burke, R. Mc Donagh, O. Mathieu, I. Osorio, C. Keesee, A. Morones, E. L. Petersen, W. Wang, T. A. DeVerter, M. A. Oehlschlaeger, B. Rhodes, R. K. Hanson, D. Davidson, B. W. Weber, C-J. Sung, J. Santner, Y. Ju, F. M. Haas, F. L. Dryer, E. N. Volkov, E. J. K. Nilsson, A. A. Konnov, M. Alrefae, F. Khaled, A. Farooq, P. Dirrenberger, P-A. Glaude, F. Battin-Leclerc, H. J. Curran, 162 (2015) 296-314.
20. W. K. Metcalfe, S. M. Burke, S. S. Ahmed, H. J. Curran, Int. J. Chem. Kinet. 45 (2013) 638-675.
21. M. Pelucchi, K. P. Somers, K. Yasunaga, U. Burke, A. Frassoldati, E. Ranzi, H. J. Curran, T. Faravelli, 162 (2014) 265-286.
22. J. Bugler, K. P. Somers, E. J. Silke, H. J. Curran, (2015) submitted for publication.